Hindawi
Mathematical Problems in Engineering
Volume 2022, Article ID 8523370, 8 pages
https://doi.org/10.1155/2022/8523370

Research Article

A Threshold Segmentation Algorithm for Sculpture Images Based on Sparse Decomposition

Zhao Yang[1] and Jixin Wan[2]

[1]*School of Fine Arts and Design, Yangzhou University, Yangzhou 225009, Jiangsu, China*
[2]*Xiamen Academy of Arts and Design, Fuzhou University, Xiamen 361021, Fujian, China*

Correspondence should be addressed to Jixin Wan; t04303@fzu.edu.cn

Received 14 March 2022; Accepted 3 June 2022; Published 23 June 2022

Academic Editor: Punit Gupta

Aiming at the problem of low efficiency and insufficient accuracy of threshold solution in multithreshold sculpture image segmentation, this paper proposes a threshold segmentation algorithm for sculpture images based on sparse decomposition. In this paper, sparse decomposition is introduced to optimize the model to reduce the impact of local noise on segmentation accuracy, and an energy functional based on pixel coconstraint is built to make up for the defect that pixels cannot retain local details. At the same time, the weighted sum of elite solution sets is used to determine Neighborhood centers increase communication between groups. Experiments show that compared with other algorithms, the above method has significant advantages in convergence efficiency and accuracy.

1. Introduction

The influence of images on sculpture is first and foremost a result of the shift in the manner in which art is disseminated. Public sculptures in the classical period are always placed in the heart of a city square or in front of significant buildings in order to hold the most prominent position in a city and emphasize the crucial function that sculptures play in a society. For people living throughout the classical period, these public locations where sculptures could be found were the best public places in which they could use word of mouth as a means of communication in order to gain information, spread knowledge, and investigate the truth. Because of the necessities of the colossal setting, classical sculpture allows the work to get attention and spread throughout the world. Over time, the rise of modern industrial society has eroded the monumentality and public visibility that sculpture formerly possessed. While at the same time, the growth of science and technology resulted in modern architecture bursting out with an unparalleled amount of energy. Because the interior space now has more possibilities and a greater variety of changes, modern architecture has progressively taken over the traditional role of sculpture from volume to space, and has emerged as a key player in the development of urban public space. While the public's awareness of sculpture is waning, the likelihood of it being propagated and displayed in public spaces is becoming increasingly remote as time goes on.

More sculpture works are being presented in galleries, art galleries, and museums, and they are being spread through albums as a result of the blooming of modernist art and the changing of art ecology. They have an impact on the entire public on a broad scale When the world entered the postindustrial age in the second half of the twentieth century, electronic media soon displaced text media as the major mode of information dissemination and rose to become the most influential mode of communication. These days, the rapid arrival of the Internet era has been swiftly characterized as an era of world images, in which the world has been transformed into images. People's primary source of knowledge and understanding of the world has shifted from written words to visual images. In the invasion and transformation of art discourse, the features of image distribution have been increasingly important in recent years.

The sculpture as a three-dimensional art form must make adjustments and new alterations to some notions and principles that have been established since the classical period in order to get access to today's popular communication by absorbing some visual experience of images.

Image segmentation (IS) is a fundamental and difficult scientific issue to understand. As a critical link in the image processing chain, the accuracy of picture target extraction and recognition, as well as the effectiveness of future work, are all influenced by the quality of segmentation performed. Because of its simplicity and efficacy, threshold segmentation is commonly employed in picture segmentation [1–8]. IS is a technique for dividing an image into several sections, each having a distinct meaning, in order to retrieve the portion of interest for further investigation. One of the most important methods in IS, the ACM model, has been widely applied in CV, PR, target tracking, and a variety of other applications. In recent years, with the advancement of NN, the combination of deep learning and active contour models has become increasingly popular for solving complicated segmentation and recognition challenges in medical pictures. Deep learning and active contour models are being used by some researchers to autonomously segment the left ventricle from magnetic resonance imaging data. It is possible to separate active contour models into two types: active contour models based on global information and active contour models based on local information [9–14].

3D feature extraction and automatic reconstruction of sparse image sequences using 3D feature reconstruction and sparse scattered point structure reorganization methods are becoming more common as 3D image processing technology advances. These methods can improve the automatic resolution and feature recognition capabilities of sparse image sequences as 3D feature reconstruction and sparsely scattered point structure reorganization methods become more common. In this paper, we investigate the 3D reconstruction method of the sparse image sequence, and we combine the adaptive feature reconstruction (AFR) of image and the point cloud data analysis method in order to realize the AFR of the sparse image sequence and improve the automatic recognition and detection ability of sparse images. Research in related image processing technology is extremely important in the disciplines of medical image processing, artificial intelligence recognition, and remote detection, among other applications [15–24].

It is more robust to picture segmentation results with big disparities in foreground and background gray levels when the CV model is used, but it is more sensitive to high noise when the CV model is used. Value filtering and Gaussian filtering are used to regularize the level set technique. To punish the level set function as a binary function, the level set function is first transformed into a Gaussian smoothing kernel and then regularized. This method combines the advantages of the CV model with the characteristics of local and global segmentation to provide a powerful tool for data analysis [25–30]. The SPF function is created to drive the contour evolution, which enhances the model's resistance to noise by increasing the number of iterations. The model, on the other hand, is sensitive to the position of the beginning contour, and it is simple to slip into the local optimum early, failing to catch the remote target during the evolution of the active contour during its evolution. Other researchers have proposed a saliency-driven top-down level set model of the region edge as a solution to this problem. Incorporating the saliency feature map and color gray level to produce energy functional, this model, which is based on the CV model, increases the extraction of the model from complex backdrops. As a result of the model's reliance on saliency maps, it is sensitive to changes in visual noise and intensity, among other things [31–38].

As a result, the level set IS model's segmentation results are not accurate enough and are sensitive to the beginning contour position and noise, and the threshold solution efficiency and accuracy in multithreshold sculpture IS are both low. It is proposed in this paper that a threshold segmentation technique for sculpture images based on sparse decomposition be used to segment sculpture photos. It is necessary to first introduce the pixel extraction picture block information in order to develop a symbolic pressure function in order to prevent the contour from becoming stuck in its local optimum during the evolution phase. To compensate for the fact that superpixels are incapable of preserving local features, a new energy functional based on pixel coconstraints is developed. Additionally, this document introduces, for the purpose of optimizing the model, a sparse decomposition method which is applied to limit the impact of local noise on segmentation accuracy.

2. Visualization of Sculpture

2.1. The Reason for the Change. One of the most prevalent problems facing conventional visual art in modern times is that a single professional knowledge base cannot keep up with the rapid development of modern society, which has seen everything from printing to video to interactive media in the last several decades. An increase in this kind of development is sufficient evidence that the nature of art culture is shifting from verbal to visual culture. It is more important for the public that the sculptural culture be aesthetically pleasing to the eye rather just providing traditional visual stimulation. Sculpture, when viewed through the eyes of someone who is accustomed to seeing images, can appear dull due to the monotonous colors used in its creation. As a result, space art that has lost its visual experience will be unable to convey its original appeal. In this setting, the sculpture will move in a direction of visualization that is extremely distinct from the typical orientation of the discipline.

2.2. Performance of Transformation. Rodin's prognosis is now a reality, and sculpture has undergone profound transformations in the setting of visual culture as a result. The French scholar Baudrillard once divided cultural history since the Renaissance into three stages based on changes in the symbolic representation system: the first stage was the classical cultural period, during which imitation served as the primary paradigm and which lasted from the Renaissance to

the Industrial Revolution; the second stage was the modern cultural period, during which imitation served as the primary paradigm and which lasted from the Renaissance to the Industrial Revolution; the third stage was the postmodern cultural period, which lasted from the Renaissance to the Industrial Revolution. The recreation of natural phenomena was during the Industrial Revolution that the second stage emerged, which was characterized by a production-oriented mindset. These days, symbols are not only restricted to the imitation of reality but also possess a certain degree of autonomy in their own right. The third stage is referred to as digital control and is the current dominant paradigm in the simulacrum stage, and symbols have complete autonomy, manufacturing, and replicating according to their own logic in order to create virtual reality. The third stage, sometimes known as the visual culture stage, is concerned with the cultural context of the current artist's creation.

Visual culture can be defined as the representation of culture in visual form. There are no restrictions on how it can be used in the sphere of visual art. Visual phenomena have spread to every sphere of social life, encompassing everything from prints, television images, and mobile phone interfaces to architectural styles and urban visual images, among other things. The characteristics of this era are as follows: the dominant mode of understanding the world is not through direct touch with the real world but rather through indirect interaction with the real world through watching and experiencing images. According to Heidegger, in essence, the world image does not refer to a vision of the world but rather to the world as it is comprehended as an image by the individual.

2.2.1. Color Realization of Sculpture. Many contemporary sculpture artists place a strong emphasis on the use of color in their work. Because traditional sculpture is regarded as the art of mixing material and space, a single hue can usually be used to better showcase the texture of the sculpture material in order to attract the attention of onlookers. As a result, when it comes to creating, color is not the most important consideration for artists. Since the beginning of the Renaissance, sculptures built by artists have been painted only on a few occasions, despite the fact that there has been a creative way of painting sculptures since ancient times. A single form of color expression was substituted for the use of multiple colors in sculpture at that time, in order to better portray the spiritual appeal of classicism and put the audience in a state of concentration. However, the rationale behind this aesthetic style does not allow it to match the visual aesthetic standards of the contemporary public. Once the artist has painted the sculpture with a variety of colors, the texture of the sculptural material itself no longer has the expressiveness of the past. If you look at modern sculpture's link between fishing and form, in particular, the shape of the sculpture is frequently exhibited with vivid colors in order to provide sufficient preparations for the ultimate color presentation. As a result, when we look at photographs of these sculptures, we have no way of knowing if the photographer is photographing a sculpture or a painting.

2.2.2. Image Expression of Sculpture. The trend of "imagination" can be seen in sculptural works created in the context of current people's visual culture. The usage of images as inspiration for artists to produce sculptures can be said to be a given, and images are also closely associated with the materials that are used in the construction of artistic sculptures. A sculpture is first and foremost an artistic creation based on a certain image. A sculpture, from a specific point of view, is a three-dimensional representation of an idea in three dimensions. In traditional sculpture creation, artists are frequently inspired by the real world; some of these inspirations are objects found in nature, while others are the hands of humans. Crafts, for example, the sculptural artist Rodin is preoccupied with the human body, and the artist Henry is obsessed with the many forms of coastal pebbles, all of which might express a specific relationship between the sculptural artist and the world in which they live. As a result of this shift in aesthetic perceptions, sculpting artists are no longer able to draw the resources needed for production from their surroundings and are instead turning to various pictures recognized by the general public to obtain those resources needed for creation. That is to say, when artists create sculptures, they frequently draw inspiration from cultures in the developing world and transform flat pictures into three-dimensional artistic forms of expression. Wang Du, a sculptor who lives in France, is a good example of this. The artist transforms a specific image seen in magazines and newspapers into a three-dimensional creative sculpture with the use of digital technology. The prominent sculpture artist Xu Hongfei was influenced by the Guangzhou Daily and developed a series of sculpture works with the motivation of creating "Lovely Soldier," which had a significant impact on the area of art.

2.2.3. The Presentation Method of Sculpture. In the world of contemporary art, the sculpture is seen as a notion that is extremely open to interpretation. For example, the iconic piece "Spiral Breakwater" by artist Robert Smith, as well as artist Heizer's book "Double Negative," are both considered works of art. Because of different limits in terms of space and time, some ordinary audiences are unable to access the world of sculpture art at all; additionally, because these works of art are on a monumental scale, even those audiences who are present at the sculpture site are unable to use a typical camera. The piece can only be seen in its whole if viewed from a specific angle, and only through an image captured from that specific angle can you appreciate its complete face. As a result, the works generated by these writers are frequently offered to the public through contemporary means such as photographs and videos. Therefore, the image is vital in the understanding of sculptures and is crucial and decisive in the process of distributing the art form, according to this point of view.

3. Method

First of all, this paper introduces the traditional segmentation method, CV model, LIF model, and SBGFRLS method. The energy function of the CV model is

$$E^{cv}(\alpha, a_1, a_2) = \sum_{i=1}^{2} \lambda_i \int e_i(x)\mathrm{d}s, \tag{1}$$

where λ_i is the weight index, a_1 and a_2 are the average pixel intensity values inside and outside the curve, and $e_1(x)$ and $e_2(x)$ are

$$e_1^{cv}(x) = \left|I - a_1\right|^2 H(\alpha), \tag{2}$$

$$e_2^{cv}(x) = \left|I - a_2\right|^2 (1 - H(\alpha)), \tag{3}$$

where $H(\alpha)$ is the Heaviside function.

The energy function of the LIF model is

$$E^{lif}(\alpha) = \frac{1}{2} \int_{\Omega} \left|I(x) - I^{lif}(x)\right|^2 \mathrm{d}x, \tag{4}$$

where $x \in \Omega$ and the local image fitting formula is

$$I^{lif} = b_1 H_\varepsilon(\alpha) + b_2 (1 - H_\varepsilon(\alpha)), \tag{5}$$

where

$$b_1 = \text{average}\left(I \in \{x \in \Omega | \alpha(x) < 0\} \cap W_k(x)\right), \tag{6}$$

$$b_2 = \text{average}\left(I \in \{x \in \Omega | \alpha(x) > 0\} \cap W_k(x)\right). \tag{7}$$

The symbolic pressure function of SBGFRLS is

$$spf(I(x)) = \frac{I(x) - (a_1 + a_2/2)}{\max\left(I(x) - (a_1 + a_2/2)\right)}. \tag{8}$$

The evolution equation of SBGFRLS is

$$\frac{\partial \alpha_p}{\partial t} = spf(I(x)) \times \left(\text{div}\left(\frac{\nabla \alpha_p}{\left|\nabla \alpha_p\right|}\right) + \beta\right) + \nabla spf(I(x)) \times \nabla \alpha. \tag{9}$$

ACM based on global information can handle images with simple intensity information well, but ACM based on local information may be used to extract targets from complicated scenes with more image details, and both methods are effective. As a result, integrating image local information with ACM-based global information can increase the segmentation ability of ACM-based global information.

Next, we introduce the OTSU segmentation method. OTSU can help us determine the threshold. The probability p_i that a pixel appears in the image is

$$p_i = \frac{f_i}{M \times N}, \quad \sum_{i=0}^{L-1} p_i = 1 \tag{10}$$

Set the threshold combination as $[t_1, t_2, \cdots, t_k]$ to divide the image into $K+1$ regions. Then, the proportion w_i and average gray level u_i of each area are

$$\begin{cases} w_0 = \sum_{i=0}^{t_1-1} p_i, w_1 = \sum_{i=t_2}^{t_2-1} p_i \\ \vdots \\ w_k = \sum_{i=t_k}^{L-1} p_i \end{cases} \tag{11}$$

$$\begin{cases} u_0 = \sum_{i=0}^{t_1-1} \frac{i p_i}{w_0}, u_1 = \sum_{i=t_2}^{t_2-1} \frac{i p_i}{w_1} \\ \vdots \\ u_k = \sum_{i=t_k}^{L-1} \frac{i p_i}{w_k} \end{cases} \tag{12}$$

Let u_t be the average gray level of the image; then, the interclass variance is expressed as

$$\sigma_B^2(t_1, t_2, \cdots t_k) = \sum_{i=0}^{k} w_i \times \left(u_j - u_t\right)^2. \tag{13}$$

$$u_t = \sum_{i=0}^{L-1} i p_i. \tag{14}$$

ACM only evaluates the global information of the image throughout the process of contour evolution, which makes it simple to fall into local optimum and to be affected by noise in the process of contour evolution. However, introducing local image information into ACM on the basis of global information requires a significant amount of iterative time. The superpixel algorithm is a widely used image preprocessing algorithm that divides an image into several visually meaningful and spatially disjoint regions while retaining the effective information of the image for more in-depth image analysis. It divides an image into several visually meaningful and spatially disjoint regions while retaining the effective information of the image for more in-depth image analysis. It performs an analysis while at the same time preserving the boundary information of the target in the image. Given that superpixels retain the image's nonglobal information, the use of superpixels in the segmentation process can reduce the influence of local grayscale differences on contour evolution, improve the segmentation accuracy of the image, and reduce the amount of computation required to accelerate the evolution of contours in the image. Simple linear iterative clustering is one of the most extensively used superpixel segmentation methods currently available, owing to its quick running time and ability to maintain ideal outlines in the image. Calculating the pixel gray difference between pixels and centroids is accomplished through the usage of the metric function. In addition to distance difference, a clustering operation is conducted on pixels, and a small number of superpixels is utilized to describe picture attributes in place of a large number of

pixels, therefore reducing the complexity of image processing.

We further introduce superpixels, and the pressure function in this paper is

$$spf\left(I_{\text{our}}(x)\right) = \frac{I_{\text{our}}(x) - (a_1 + a_2/2)}{\max\left(I_{\text{our}}(x) - (a_1 + a_2/2)\right)}, \tag{15}$$

$$I_{\text{our}}(x) = \sum_{l=1}^{K} \text{Average}(I_l). \tag{16}$$

Although superpixels keep the regional information of an image and can make greater use of the link between distant pixels, relying solely on superpixel features to preserve picture details would result in a loss of image details. As a result, when the superpixel is undersegmented, it is possible that the target contour will not be accurately retrieved. We present an IS approach based on pixel/superpixel cooperative constraints in this study in order to compensate for the flaw that a single superpixel is incapable of preserving local features. Sparse constraints are included in the model in order to reduce the influence of oversegmentation and local noise on contour evolution, and the evolution equations are provided in equations (17) and (18) to illustrate how this is accomplished.

$$\frac{\partial \alpha_p}{\partial t} = spf(I(x)) \times \left(\text{div}\left(\frac{\nabla \alpha_p}{\left|\nabla \alpha_p\right|}\right) + \beta\right) + \nabla spf(I(x)) \times \nabla \alpha_p, \tag{17}$$

$$\begin{aligned}\frac{\partial \alpha_{\text{sup}}}{\partial t} &= \omega \times spf\left(I_{\text{sup}}(x)\right) \times \left(\text{div}\left(\frac{\nabla \alpha_{\text{sup}}}{\left|\nabla \alpha_{\text{sup}}\right|}\right) + \beta\right) \\ &\quad + \nabla spf\left(I_{\text{sup}}(x)\right) \times \nabla \alpha_{\text{sup}} \\ &\quad + \mu \times \frac{\left(\partial \alpha_p/\partial t\right) - \min\left(\partial \alpha_p/\partial t\right)}{\max\left(\partial \alpha_p/\partial t\right) - \min\left(\partial \alpha_p/\partial t\right)}.\end{aligned} \tag{18}$$

Equations (17) and (18) can be simplified to

$$\frac{\partial \alpha_p}{\partial t} = spf(I(x)) \cdot \left|\nabla \alpha_p\right|, \tag{19}$$

$$\begin{aligned}\frac{\partial \alpha_{\text{sup}}}{\partial t} &= \omega \cdot spf\left(I_{\text{sup}}(x)\right) \cdot \left|\nabla \alpha_p\right| + \mu \\ &\quad \times \frac{\left(\partial \alpha_p/\partial t\right) - \min\left(\partial \alpha_p/\partial t\right)}{\max\left(\partial \alpha_p/\partial t\right) - \min\left(\partial \alpha_p/\partial t\right)}.\end{aligned} \tag{20}$$

Furthermore, this paper introduces a sparse decomposition method to solve the scaled coordinates.

$$x_{k+1} = x_k + \gamma R_e x_k, \tag{21}$$

$$x_{k+1} = x_k + \varsigma R_a x_k, \tag{22}$$

where R_a is a sparse random diagonal matrix with nonzero values from a standard normal distribution.

Using the local mean noise reduction approach, the collected original three-dimensional sculpture point sparse image is isolated from noise. The feature points' thresholds are then set, and the noise separation processing is carried out in accordance with the threshold judgment result. The feature point set that has been formed is as follows:

Figure 1: Original image cloud feature sampling.

$$\begin{pmatrix} x & y & z \\ 0 & 0 & 0 \end{pmatrix} = \begin{pmatrix} (H + \tau \cdot I) & P \\ P^T & O \end{pmatrix} \begin{pmatrix} \gamma & \theta & \omega \\ a & b & c \end{pmatrix}. \tag{23}$$

4. Sculpture Image Threshold Segmentation (SITS)

The simulation experiment analysis is carried out in this research in order to evaluate the performance of the threshold segmentation algorithm of a sculptured picture based on sparse decomposition in terms of performance. For the experiment, the MATLAB simulation tool is used to design the experiment, and Visual Studio 2020 is used to create the image processing software platform for the 3D reconstruction of sparsely scattered points. The pixels collected for sparse images of sculpture points are 20 million, the number of connection points of feature lines is 500, and the feature resolution is 640×400, the interference noise is Gaussian noise, and the intensity is -12 dB. The original point cloud feature sample is achieved as illustrated in Figure 1 using the simulation parameter settings described above.

Using the sampled image in Figure 2 as input, the detection result is shown in Figure 1. The three-dimensional point cloud feature of the sculpture point sparse image is detected and shown in Figure 3.

The gradient operation method is used to decompose the feature detected in Figure 3 as the input of the threshold segmentation of the sculpture point image, and the information enhancement and fusion filtering of the sparse image of the sculpture point are realized, and the image is reconstructed, and the reconstructed output is obtained as shown in Figure 4.

JS and Dice coefficients are employed in order to study and evaluate the segmentation quality of the suggested SITS model. This allows us to validate the effectiveness of our strategy.

The JS and DICE values for the four approaches are depicted in Figures 5 and 6, respectively. It can be observed

Figure 2: Edge profile feature.

Figure 3: Sparse scattered point features.

Figure 4: Sculpture image reconstruction output.

in Figures 5 and 6 that CV and LIF are susceptible to strong noise and weak boundaries; their average JS values are 0.845 and 0.869, and their average DICE values are 0.848 and 0.788, respectively, indicating that they are susceptible to strong noise and weak boundaries. The SBGFRLS model is

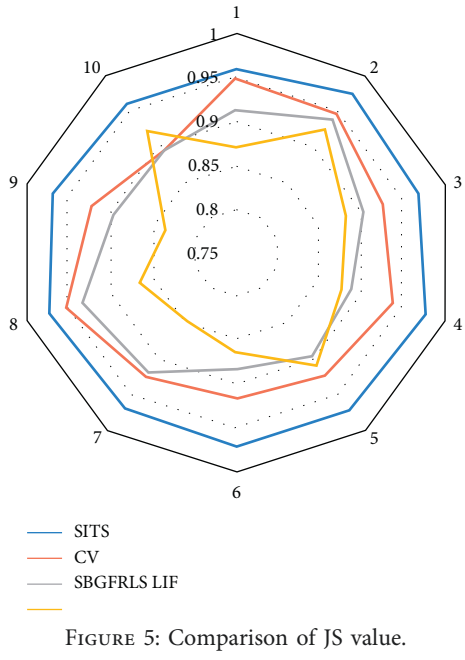

Figure 5: Comparison of JS value.

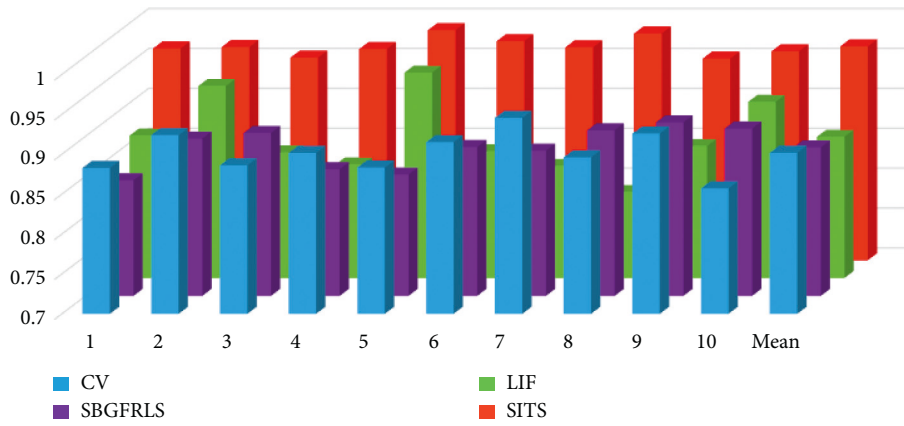

Figure 6: Comparison of DICE value.

unable to capture pixels at the extreme end of the spectrum. As a result of this, the relationship between them is susceptible to falling into a local maximum, with an average JS value of 0.715 in the experiment.

5. Conclusion

In order to address the issue that the segmentation results of the sculpture IS model are not accurate enough and are sensitive to the initial contour position and noise, this paper proposes a threshold segmentation algorithm for sculpture images based on sparse decomposition. This algorithm realizes the adaptive structural reorganization of sparse image sequences and improves the automatic processing of sparse images by reducing the sensitivity to the initial contour position and noise with the ability to identify and notice potential dangers. In order to address the issue of sluggish evolution of the active contour model based on nonglobal information, the model makes use of superpixel blocks to accelerate the evolution of the active contour model. The findings of this study demonstrate that the method described in this paper requires less prior knowledge for sculptural picture segmentation, and that both the JC and DICE indicators perform much better than traditional comparison methods.

Data Availability

The data used to support the findings of this study are available from the corresponding author upon request.

Conflicts of Interest

The authors declare that they have no conflicts of interest.

Acknowledgments

The paper was supported by the project source: Research on the Improvement path of the quality of urban humanistic landscape from the perspective of public cultural service and fund project: supported by the Humanities and Social Sciences Foundation of Yangzhou University, Project No.: 26.

References

[1] Y. Xue, X. Guo, and X. Cao, "Motion saliency detection using low-rank and sparse decomposition," in *Proceedings of the 2012 IEEE international conference on acoustics, speech and signal processing (ICASSP)*, pp. 1485–1488, IEEE, Kyoto, Japan, March 2012.

[2] X. Shen and Y. Wu, "A unified approach to salient object detection via low rank matrix recovery," in *Proceedings of the 2012 IEEE Conference on Computer Vision and Pattern Recognition*, pp. 853–860, IEEE, Providence, RI, USA, June 2012.

[3] H. Mohimani, M. Babaie-Zadeh, and C. Jutten, "A fast approach for overcomplete sparse decomposition based on smoothed $\ell{0} $ norm," *IEEE Transactions on Signal Processing*, vol. 57, no. 1, pp. 289–301, 2008.

[4] C. Shi, Y. Cheng, J. Wang, Y. Wang, K. Mori, and S. Tamura, "Low-rank and sparse decomposition based shape model and probabilistic atlas for automatic pathological organ segmentation," *Medical Image Analysis*, vol. 38, pp. 30–49, 2017.

[5] H. Peng, B. Li, H. Ling et al., "Salient object detection via structured matrix decomposition," *IEEE Transactions on Pattern Analysis and Machine Intelligence*, vol. 39, no. 4, pp. 818–832, 2016.

[6] M. D. Collins, J. Xu, L. Grady et al., "Random walks based multi-image segmentation: quasiconvexity results and gpu-based solutions," in *Proceedings of the 2012 IEEE Conference on Computer Vision and Pattern Recognition*, pp. 1656–1663, IEEE, Providence, RI, USA, June 2012.

[7] J. Pont-Tuset, P. Arbelaez, and J. T. Barron, "Multiscale combinatorial grouping for image segmentation and object proposal generation," *IEEE Transactions on Pattern Analysis and Machine Intelligence*, vol. 39, no. 1, pp. 128–140, 2016.

[8] R. Xia, Y. Pan, and L. Du, "Robust multi-view spectral clustering via low-rank and sparse decomposition," *Proceedings of the AAAI Conference on Artificial Intelligence*, vol. 28, no. 1, 2014.

[9] J.-L. Starck, M. Elad, and D. L. Donoho, "Image decomposition via the combination of sparse representations and a variational approach," *IEEE Transactions on Image Processing*, vol. 14, no. 10, pp. 1570–1582, 2005.

[10] B. Trémoulhéac, N. Dikaios, and D. Atkinson, "Dynamic MR image reconstruction–separation from undersampled (${\bf k}, t $)-Space via low-rank plus sparse prior," *IEEE Transactions on Medical Imaging*, vol. 33, no. 8, pp. 1689–1701, 2014.

[11] I. Ramirez, P. Sprechmann, and G. Sapiro, "Classification and clustering via dictionary learning with structured incoherence and shared features," in *Proceedings of the 2010 IEEE Computer Society Conference on Computer Vision and Pattern Recognition*, pp. 3501–3508, IEEE, San Francisco, CA, USA, June 2010.

[12] J. Funke, F. Tschopp, and W. Grisaitis, "Large scale image segmentation with structured loss based deep learning for connectome reconstruction," *IEEE Transactions on Pattern Analysis and Machine Intelligence*, vol. 41, no. 7, pp. 1669–1680, 2018.

[13] F. Sultana, A. Sufian, and P. Dutta, "Evolution of image segmentation using deep convolutional neural network: a survey," *Knowledge-Based Systems*, vol. 201-202, Article ID 106062, 2020.

[14] M. Elad and M. Aharon, "Image denoising via sparse and redundant representations over learned dictionaries," *IEEE Transactions on Image Processing*, vol. 15, no. 12, pp. 3736–3745, 2006.

[15] E. Imani, M. Javidi, and H.-R. Pourreza, "Improvement of retinal blood vessel detection using morphological component analysis," *Computer Methods and Programs in Biomedicine*, vol. 118, no. 3, pp. 263–279, 2015.

[16] W. Sun, C. Liu, J. Li, Y. M. Lai, and W. Li, "Low-rank and sparse matrix decomposition-based anomaly detection for hyperspectral imagery," *Journal of Applied Remote Sensing*, vol. 8, no. 1, Article ID 083641, 2014.

[17] W. Hu, Y. Yang, and W. Zhang, "Moving object detection using tensor-based low-rank and saliently fused-sparse decomposition[J]," *IEEE Transactions on Image Processing*, vol. 26, no. 2, pp. 724–737, 2016.

[18] J. Mairal, F. Bach, and J. Ponce, "Online dictionary learning for sparse coding," in *Proceedings of the 26th annual international conference on machine learning*, pp. 689–696, Montreal, Quebec, Canada, June 2009.

[19] W. Weisheng Dong, L. Lei Zhang, G. Guangming Shi, and fnm Xiaolin Wu, "Image deblurring and super-resolution by adaptive sparse domain selection and adaptive regularization," *IEEE Transactions on Image Processing*, vol. 20, no. 7, pp. 1838–1857, 2011.

[20] X. Fu, Z. J. Zha, and F. Wu, "Jpeg artifacts reduction via deep convolutional sparse coding," in *Proceedings of the IEEE/CVF International Conference on Computer Vision*, pp. 2501–2510, Seoul, Korea, October 2019.

[21] D. Liu, Z. Wang, B. Wen, J. Yang, W. Han, and T. S. Huang, "Robust single image super-resolution via deep networks with sparse prior," *IEEE Transactions on Image Processing*, vol. 25, no. 7, pp. 3194–3207, 2016.

[22] R. A. Borsoi, T. Imbiriba, and J. C. M. Bermudez, "A fast multiscale spatial regularization for sparse hyperspectral unmixing," *IEEE Geoscience and Remote Sensing Letters*, vol. 16, no. 4, pp. 598–602, 2018.

[23] X. Pan, L. Li, H. Yang et al., "Accurate segmentation of nuclei in pathological images via sparse reconstruction and deep convolutional networks," *Neurocomputing*, vol. 229, pp. 88–99, 2017.

[24] Z. Huang, X. Wang, and J. Wang, "Weakly-supervised semantic segmentation network with deep seeded region growing," in *Proceedings of the IEEE conference on computer vision and pattern recognition*, pp. 7014–7023, IEEE, Lake City, UT, USA, June 2018.

[25] X. Yu, T. Liu, and X. Wang, "On compressing deep models by low rank and sparse decomposition," in *Proceedings of the IEEE Conference on Computer Vision and Pattern Recognition*, pp. 7370–7379, IEEE, Honolulu, HI, USA, July 2017.

[26] H. Zhu, F. Meng, J. Cai, and S. Lu, "Beyond pixels: a comprehensive survey from bottom-up to semantic image segmentation and cosegmentation," *Journal of Visual Communication and Image Representation*, vol. 34, pp. 12–27, 2016.

[27] C. Yan, Z. Li, Y. Zhang, Y. Liu, X. Ji, and Y. Zhang, "Depth image denoising using nuclear norm and learning graph model," *ACM Transactions on Multimedia Computing, Communications, and Applications*, vol. 16, no. 4, pp. 1–17, 2020.

[28] L. Hou, D. Samaras, and T. M. Kurc, "Patch-based convolutional neural network for whole slide tissue image classification," in *Proceedings of the IEEE conference on computer vision and pattern recognition*, pp. 2424–2433, IEEE, Honolulu, HI, USA, October 2016.

[29] S. Javed, A. Mahmood, T. Bouwmans, and S. K. Jung, "Background-foreground modeling based on spatiotemporal sparse subspace clustering," *IEEE Transactions on Image Processing*, vol. 26, no. 12, pp. 5840–5854, 2017.

[30] A. Heshmati, M. Gholami, and A. Rashno, "Scheme for unsupervised colour-texture image segmentation using neutrosophic set and non-subsampled contourlet transform," *IET Image Processing*, vol. 10, no. 6, pp. 464–473, 2016.

[31] Y. Qian and M. Ye, "Hyperspectral imagery restoration using nonlocal spectral-spatial structured sparse representation with noise estimation," *Journal of Selected Topics in Applied Earth Observations and Remote Sensing*, vol. 6, no. 2, pp. 499–515, 2012.

[32] C. Scharfenberger, A. Wong, and K. Fergani, "Statistical textural distinctiveness for salient region detection in natural images," in *Proceedings of the IEEE conference on computer vision and pattern recognition*, pp. 979–986, IEEE, Portland, OR, USA, June 2013.

[33] K. K. Maninis, J. Pont-Tuset, and P. Arbeláez, "Convolutional oriented boundaries: from image segmentation to high-level tasks," *IEEE Transactions on Pattern Analysis and Machine Intelligence*, vol. 40, no. 4, pp. 819–833, 2017.

[34] Z. Wang, D. Liu, and J. Yang, "Deep networks for image super-resolution with sparse prior," in *Proceedings of the IEEE international conference on computer vision*, pp. 370–378, IEEE, Santiago, Chile, December 2015.

[35] W. Ren, J. Tian, and Z. Han, "Video desnowing and deraining based on matrix decomposition," in *Proceedings of the IEEE Conference on Computer Vision and Pattern Recognition*, pp. 4210–4219, IEEE, Honolulu, HI, USA, July 2017.

[36] L. Shao, R. Yan, and X. Li, "From heuristic optimization to dictionary learning: a review and comprehensive comparison of image denoising algorithms," *IEEE Transactions on Cybernetics*, vol. 44, no. 7, pp. 1001–1013, 2013.

[37] T. Blaschke, C. Burnett, and A. Pekkarinen, "Image segmentation methods for object-based analysis and classification," *Remote Sensing Image Analysis: Including the Spatial Domain*, Springer, Dordrecht, pp. 211–236, 2004.

[38] L. Garcia Ugarriza, E. Saber, S. R. Vantaram, V. Amuso, M. Shaw, and R. Bhaskar, "Automatic image segmentation by dynamic region growth and multiresolution merging," *IEEE Transactions on Image Processing*, vol. 18, no. 10, pp. 2275–2288, 2009.